

## New neutrino-nucleus reaction cross sections at solar, reactor and supernova neutrino energies

Toshio Suzuki<sup>1,a</sup>, Michio Honma<sup>2</sup>, A. B. Balantekin<sup>3</sup>, Toshitaka Kajino<sup>4</sup>, and Satoshi Chiba<sup>5</sup>

<sup>1</sup>Department of Physics, College of Humanities and Sciences, Nihon University, Sakurajosui 3-25-40, Setagaya-ku, Tokyo 156-8550, Japan

<sup>2</sup>Center for Mathematical Sciences, University of Aizu, Aizu-Wakamatsu, Fukushima 965-8580, Japan

<sup>3</sup>Department of Physics, University of Wisconsin, Madison, WI 53706, USA

<sup>4</sup>National Astronomical Observatory of Japan, 2-21-1 Osawa, Mitaka, Tokyo 181-8588, Japan

Department of Astronomy, School of Science, University of Tokyo, Hongo, Tokyo 113-0033, Japan

<sup>5</sup>Research Laboratory for Nuclear Reactors, Tokyo Institute of Technology, Ookayama 2-12-1, Meguro-ku, Tokyo 152-8550, Japan

**Abstract.** Remarkable improvements in the evaluation of neutrino-nucleus reaction cross sections are obtained based on new shell-model Hamiltonians with proper tensor components. New  $\nu$ -induced reaction cross sections on  $^{12}\text{C}$ ,  $^{13}\text{C}$ ,  $^{56}\text{Fe}$ ,  $^{56}\text{Ni}$  and  $^{40}\text{Ar}$  are presented, and predictions for nucleosynthesis in supernova explosions,  $\nu$ -oscillation effects and low-energy reactor and solar neutrino detection are discussed based on these new cross sections.

### 1 Introduction

Considerable improvements in the evaluations of neutrino-nucleus reaction cross sections have been achieved based on new shell-model Hamiltonians at solar, reactor and supernova neutrino energies. New shell-model Hamiltonians can successfully describe spin responses in nuclei and explain shell evolutions toward drip-lines. A common feature of the new interactions is that they have proper tensor components.

A new shell-model Hamiltonian for  $p$ -shell nuclei, SFO[1], is used to evaluate  $\nu$ - $^{12}\text{C}$  and  $\nu$ - $^{13}\text{C}$  cross sections[2–4]. The reaction cross sections on  $^{12}\text{C}$  at DAR (decay-at-rest pion) energies are shown to be well reproduced by shell-model calculations. Implications on light element synthesis such as  $^{11}\text{B}$  and  $^7\text{Li}$  in supernova explosions and effects of neutrino oscillations are discussed. A possible determination of the oscillation parameters, in particular, the mass hierarchy from the abundance ratio of  $^7\text{Li}/^{11}\text{B}$  is proposed[3, 5].  $^{13}\text{C}$  is shown to be an attractive target for detecting very low-energy neutrinos below 13 MeV with scintillator based experiments[4].

A new shell-model Hamiltonian for  $pf$ -shell nuclei, GXPF1J[6], is shown to reproduce  $\nu$ - $^{56}\text{Fe}$  cross section for DAR neutrinos[7]. It describes also well the Gamow-Teller (GT) strengths in Ni isotopes, in particular  $^{56}\text{Ni}$ [8, 9]. Neutral-current reactions on  $^{56}\text{Ni}$  are evaluated, and the enhancement of proton-emission cross sections and production of  $^{55}\text{Mn}$  element in supernova explosions are discussed[8].

---

<sup>a</sup>e-mail: suzuki@phys.chs.nihon-u.ac.jp

A liquid argon detector is a powerful tool to measure solar and supernova neutrinos. GT strength in  $^{40}\text{Ar}$  is studied by shell-model calculations with a monopole-based universal interaction[10], which has tensor components of  $\pi + \rho$  meson exchanges. GT strength in  $^{40}\text{Ar}$  and the charged-current reaction,  $^{40}\text{Ar}(\nu_e, e^-)^{40}\text{K}$ , are evaluated [11] and compared with previous calculations. New cross section for solar neutrinos from  $^8\text{B}$  will be also presented.

Carbon isotopes are treated in Sect. 2. Results for  $^{56}\text{Fe}$  and  $^{56}\text{Ni}$  are shown in Sect. 3.  $^{40}\text{Ar}$  is discussed in Sect. 4. A summary is given in Sect. 5.

## 2 $\nu$ -induced reactions on $^{12}\text{C}$ and $^{13}\text{C}$

### 2.1 $\nu$ -induced reactions on $^{12}\text{C}$ and synthesis of light elements

We constructed a new shell-model Hamiltonian, SFO[1], starting from Cohen-Kurath (CK) and Millener-Kurath (MK) interactions by enhancing monopole terms of matrix elements for  $p_{1/2}$ - $p_{3/2}$  orbits with isospin  $T=0$ . Systematic improvements in the description of magnetic moments of  $p$ -shell nuclei, reproduction of GT transitions in  $^{12}\text{C}$  and  $^{14}\text{C}$  are obtained with configuration space including up to  $2\hbar\omega$  excitations and with the use of a small quenching of the axial-vector coupling constant and spin  $g$ -factor;  $g_A^{eff}/g_A = g_s^{eff}/g_s = 0.95$ . The SFO is found to have proper tensor components consistent with the general sign rule for the tensor-monopole terms[12], and can explain the change of the magic number from 8 to 6 toward the neutron-drip line.

The SFO is applied to evaluate  $\nu$ -induced reaction cross sections at DAR energies. The cross sections for the exclusive charged-current reaction,  $^{12}\text{C}(\nu_e, e^-)^{12}\text{N}(1^+_{g.s.})$ , obtained by SFO and CK-MK (PSDMK2[13]) are shown in figure 1 and compared with the experimental data[14]. The SFO reproduces well the experimental data. It can reproduce well both the exclusive charged-current and neutral-current reaction cross sections folded over the DAR neutrinos[2, 5]. The inclusive charged-current reaction cross section for the DAR neutrinos is also well reproduced by SFO.

The new cross sections evaluated by SFO are used for the study of light-element nucleosynthesis in supernova explosions[2, 3]. Neutral-current reactions on  $^{12}\text{C}$  and  $^4\text{He}$  are important for the production of  $^{11}\text{B}$  and  $^7\text{Li}$ . The production yields of  $^{11}\text{B}$  and  $^7\text{Li}$  are re-evaluated with the use of the new reaction cross sections of  $^{12}\text{C}$  and those of  $^4\text{He}$  obtained by WBP[15]. Calculated results are compared with previous calculations[16]. The abundances of  $^{11}\text{B}$  and  $^7\text{Li}$  evaluated by using a GCE (galactic chemical evolution) model are found to be enhanced by 13~14% compared with those by HW92[16].

### 2.2 Effects of $\nu$ -oscillation and $\nu$ -mass hierarchy

The effects of matter  $\nu$ -oscillations on the production of  $^{11}\text{B}$  and  $^7\text{Li}$  in supernova explosions are discussed. Matter oscillations in neutrinos by the MSW mechanism can occur near the O/C layer for the normal mass hierarchy case, while for anti-neutrinos the high-density resonance can occur for the inverted mass hierarchy. When there is  $\nu$ -oscillation and heavy-flavor neutrinos change into electron neutrinos with higher energies, charged-current reactions on  $^{12}\text{C}$  and  $^4\text{He}$  become important, and  $^{11}\text{B}$  and  $^7\text{Li}$  are produced more but the abundance ratio for  $^7\text{Li}/^{11}\text{B}$  is modified dependent on the mixing angle  $\theta_{13}$ . The dependence of the abundance ratio on  $\theta_{13}$  is shown in figure 1 for both the normal and inverted mass hierarchies. In case of normal mass hierarchy, the ratio is found to be enhanced at  $\sin^2(2\theta_{13}) > 0.002$ , where the transition is adiabatic. As the value of  $\sin^2(2\theta_{13})$  is recently determined to be around 0.1[17], we can determine the mass hierarchy from the abundance ratio of  $^7\text{Li}/^{11}\text{B}$ . Recently,  $^{11}\text{B}$  and  $^7\text{Li}$  are found in pre-solar supernova grains[18]. Using Bayesian analysis, the inverted mass hierarchy is found to be statistically more favored with a probability of 74%[19].

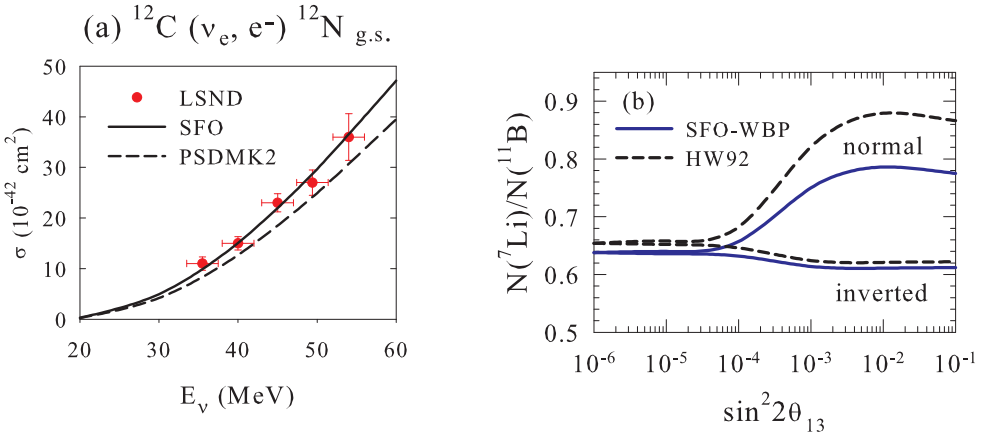


**Figure 1.** (a) Exclusive charged-current reaction cross sections on  $^{12}\text{C}$  induced by DAR neutrinos obtained for SFO and PSDMK2. Experimental values (LSND) are taken from Ref. [14]. (b) Dependence of the abundance ratio  ${}^7\text{Li}/{}^{11}\text{B}$  on the mixing angle  $\theta_{13}$  for normal and inverted  $\nu$  mass hierarchies obtained with SFO-WBP Hamiltonian set and HW92 cases[5].

**Table 1.** Calculated cross sections for  $^{13}\text{C}$  induced by solar  ${}^8\text{B}$  neutrinos. Cross sections obtained for SFO are given in units of  $10^{-43}\text{ cm}^2$

Reaction	CK	SFO
$^{13}\text{C}(\nu_e, e^-) {}^{13}\text{N}(1/2^-_{g.s.} + 3/2^- (3.50\text{ MeV}))$	10.7	13.4
$^{13}\text{C}(\nu, \nu') {}^{13}\text{C}(3/2^-, 3.69\text{ MeV})$	1.16	2.23

We are very much interested in the results of accelerator experiments on the determination of mass hierarchy in near future.

### 2.3 $\gamma$ -induced reactions on $^{13}\text{C}$

$^{13}\text{C}$  is an attractive target for very low energy neutrinos below  $E_\nu = 13\text{ MeV}$  as  $^{12}\text{C}$  can be excited only above  $E_\nu = 13\text{ MeV}$  and there is no suffering from the contamination of  $^{12}\text{C}$ . A knowledge of cross sections leading to various states in  $^{13}\text{N}$  and  $^{13}\text{C}$  would help scintillator-based searches for low-energy electron neutrinos in environments dominated by the electron antineutrinos, such as nuclear reactors.

Neutral-current and charged-current cross sections leading to low-lying states in  $^{13}\text{C}$  and  $^{13}\text{N}$  are evaluated with SFO[4]. The cross sections to excite  $3/2^-_1$  states in  $^{13}\text{C}$  and  $^{13}\text{N}$  induced by GT transitions are found to be enhanced compared to those obtained by the Cohen-Kurath interaction as shown in figure 2[20]. Calculated cross sections for solar  ${}^8\text{B}$  neutrinos are compared in table 1.

Partial cross sections for  $\gamma$  and particle emission channels are evaluated by statistical Hauser-Feshbach method to estimate the count rate for the measurement of  $\gamma$ -rays from the daughter states of the reactions. The partial cross sections for the neutral-current reaction are shown in figure 2. The detection of reactor antineutrinos would be accessible by the measurement of  $\gamma$ 's in the neutral-current reaction.

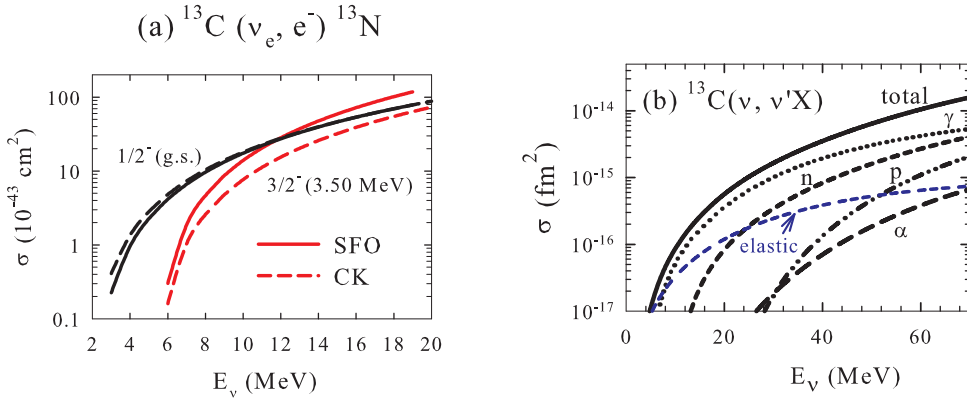


**Figure 2.** (a) Reaction cross sections for  $^{13}\text{C}(\nu_e, e^-)^{13}\text{N}$  leading to  $1/2^-_{g.s.}$  and  $3/2^-$  (3.50 MeV) states. Results for SFO and CK are compared. (b) Partial cross sections for  $^{13}\text{C}(\nu, \nu'X)$  for particle and  $\gamma$  emission channels as well as the elastic scattering obtained with SFO.

### 3 $\nu$ -induced reactions on $^{56}\text{Fe}$ and $^{56}\text{Ni}$

#### 3.1 Charged-current reaction on $^{56}\text{Fe}$

A new shell-model Hamiltonian in  $pf$ -shell, GXPF1J[6], can describe well the spin responses in  $pf$ -shell nuclei. GT strengths in Fe and Ni isotopes and magnetic dipole transition strengths in  $^{48}\text{Ca}$ ,  $^{50}\text{Ti}$ ,  $^{52}\text{Cr}$  and  $^{54}\text{Fe}$  are well reproduced with GXPF1J with a universal quenching factor of  $g_A^{eff}/g_A = 0.74$  and  $g_s^{eff}/g_s = 0.75$ .

Charged-current reaction on  $^{56}\text{Fe}$ ,  $^{56}\text{Fe}(\nu_e, e^-)^{56}\text{Co}$ , induced by DAR neutrinos is investigated. The iron target is one of few examples where experimental data are available. Calculated cross section obtained by shell-model with GXPF1J for the GT and IA transitionis and RPA for other multipoles is  $\sigma = 259 \times 10^{-42} \text{ cm}^2$ , which is close to the experimental value;  $\sigma = 256 \pm 108 \pm 43 \times 10^{-42} \text{ cm}^2$  [21]. We can now evaluate neutrino-nucleus reaction cross sections on  $^{56}\text{Fe}$  accurately with the use of the new shell-model Hamiltonian. Calculated cross sections by various methods, SM+RPA, RPA and QRPA, result in an averaged value of  $\sigma = 258 \pm 57 \times 10^{-42} \text{ cm}^2$  [7].

#### 3.2 GT strength in $^{56}\text{Ni}$ and nuclear weak processes in stars

We discuss GT strength in  $^{56}\text{Ni}$  and possible implications on nucleosynthesis of medium-mass elements. The GT strengths in Ni and Fe isotopes obtained by GXPF1J are generally more fragmented compared with those given by KB3G Hamiltonian[22]. In particular, the GT strength in  $^{56}\text{Ni}$  has two-peak structure for GXPF1J while it has a single peak for KB3G as shown in figure 3. Larger fragmentation of the GT strength in  $^{56}\text{Ni}$  for GXPF1J comes from a larger single-particle energy gap between  $0f_{5/2}$  and  $0f_{7/2}$  orbits and a larger  $T=0$  pairing strength for GXPF1J. Recent (p, n) experiment confirmed the two-peak structure of the GT strength in  $^{56}\text{Ni}$ [9].

This feature leads to smaller e-capture rates due to a smaller amount of the strength in the lower excited energy region. The e-capture rates obtained with GXPF1J, KB3G and experimental GT strength

are shown in figure 3 at stellar environments[23]. The rates are smaller for GXPF1J at high densities ( $\rho Y_e = 10^7$ - $10^9$  with  $Y_e$  the lepton to baryon ratio) and high temperatures ( $T = T_9 \times 10^9$  K) as shown in figure 3. The GXPF1J reproduces fairly well the rates for the experimental strength. Smaller e-capture rates on  $^{56}\text{Ni}$  leads to less neutron fraction in hadrons, which might help to solve the over-production problem of neutron-rich isotopes such as  $^{58}\text{Ni}$ [24].

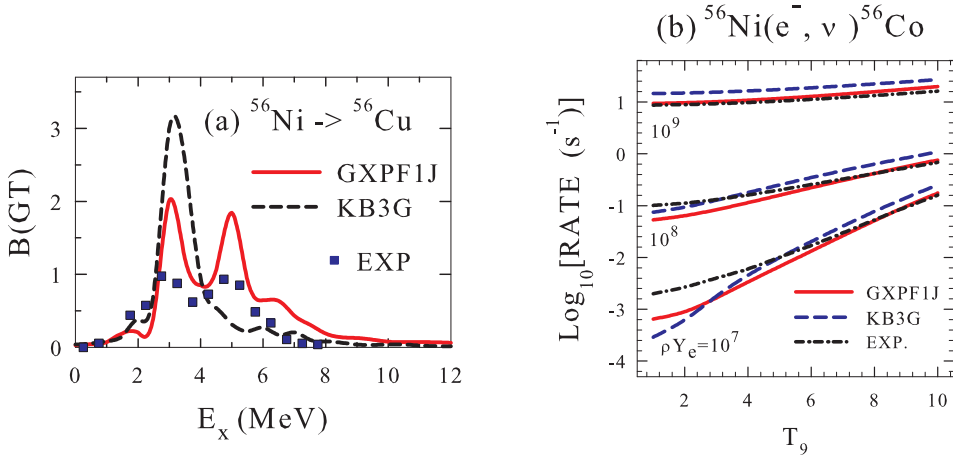


**Figure 3.** (a) GT strength in  $^{56}\text{Ni}$  for GXPF1J and KB3G. Experimental data are taken from Ref. [9]. (b) Electron capture rates on  $^{56}\text{Ni}$  obtained by GXPF1J and KB3G as well as with experimental GT strength[23].

A larger amount of the GT strength at higher excitation energy, on the other hand, leads to an enhancement of the proton-emission cross section,  $^{56}\text{Ni}(\nu, \nu' p)^{55}\text{Co}$ . This enhancement results in an enhancement of the production yield of  $^{55}\text{Mn}$  through two successive e-capture reactions on  $^{55}\text{Co}$  in population III stars (see Ref. [8] for the details).

## 4 $\nu$ -induced reactions on $^{40}\text{Ar}$

### 4.1 Monopole-based universal interaction and GT strength in $^{40}\text{Ar}$

A liquid argon detector is an excellent powerful tool to detect core-collapse supernova neutrinos. Here, we study charged-current  $\nu$ -induced reactions on  $^{40}\text{Ar}$  at solar and supernova neutrino energies. Direct measurement of the charged-current reaction cross sections are accessible by using a liquid argon time projection chamber (TPC) detector and a spallation neutron source for neutrinos.

We study GT transition strength in  $^{40}\text{Ar}$  by shell-model calculations. The SDPF-M[25] and GXPF1J[6] interactions are used for  $sd$ -shell and  $pf$ -shell, respectively. The monopole-based universal interaction (VMU)[10], which has the tensor components of  $\pi+\rho$  meson exchanges, is adopted for the  $sd$ - $pf$  cross-shell part. The bare tensor force due to  $\pi+\rho$  meson exchanges has been shown to be little modified by the renormalization procedures for both the short-range correlation and core-polarization corrections[10]. A proper inclusion of the tensor force is essential for successful description of spin-dependent modes in nuclei. The use of VMU in the  $p$ - $sd$  cross shell part of the interaction

proved to be successful in the spin modes in  $p$ - $sd$  shell nuclei[26]. The two-body spin-orbit interaction due to  $\sigma$ ,  $\omega$  and  $\rho$  meson exchanges is also added to the cross-shell part of the interaction. The interaction thus made will be referred to "SDPF-VMU" hereafter.

Calculated cumulative sum of  $B(GT)$  are shown in figure 4. Calculated values obtained by previous calculation[27] and WBT[15] as well as experimental data from (p, n) reaction[28] are also presented. Here a quenching factor of  $g_A^{eff}/g_A = 0.775$ [27] is used with configurations within  $2\hbar\omega$  excitations,  $(sd)^{-2}-(pf)^2$ . The experimental  $B(GT)$  and the cumulative sum of  $B(GT)$  are rather well described by SDPF-VMU while the strength in Ref. [27] is smaller than the observed strength. The GT strength by WBT also becomes smaller than the experimental values at larger excitation energies.

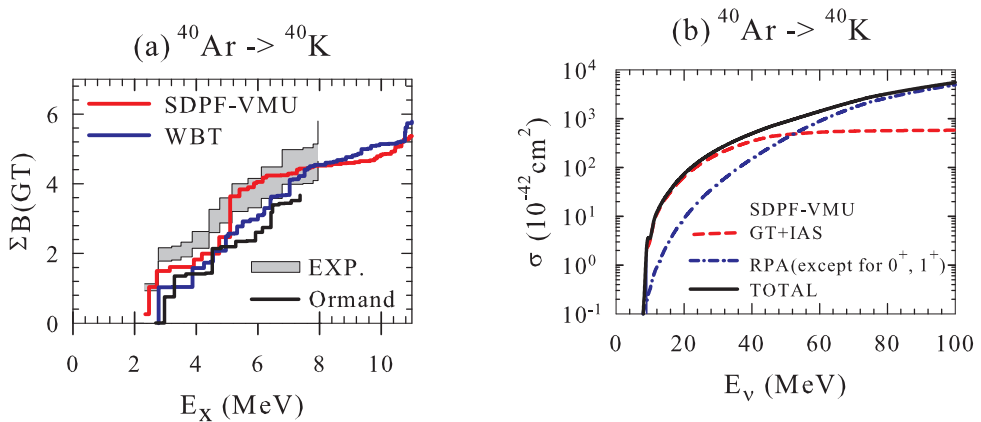


**Figure 4.** (a) Cumulative sum of  $B(GT)$  for  $^{40}\text{Ar}$  obtained with SDPF-VMU and WBT. Experimental data are taken from Ref. [28]. Results of Ref. [27] are also shown. (b) Reaction cross section for  $^{40}\text{Ar}(\nu_e, e^-)^{40}\text{K}$  obtained with SDPF-VMU for the GT and IA transitions[11]. The other multipole contributions are obtained by RPA method.

## 4.2 Charged-current reaction on $^{40}\text{Ar}$

Charged-current reaction cross sections for  $^{40}\text{Ar}(\nu_e, e^-)^{40}\text{K}$  are evaluated by shell-model calculations with SDPF-VMU for the GT ( $1^+$ ) and isobaric-analog ( $0^+$ ) transitions. Cross sections for other multipoles are obtained by RPA method as they can not be evaluated accurately by shell-model calculations with the present restricted configuration space. The contributions from spin-dipole transitions and multipoles other than  $0^+$  and  $1^+$  are found to become dominant at  $E_\nu > 50$  MeV. The calculated total cross section obtained here is found to be rather close to that in Ref. [29] obtained by RPA calculations for all the multipoles. The GT part of the present result is enhanced by about 20-40 % compared to that in Ref. [29].

Cross sections for  $^{40}\text{Ar}(\nu_e, e^-)^{40}\text{K}$  folded over  $^8\text{B}$  neutrino spectrum are shown in table 2. The cross section for the GT transition is enhanced for SDPF-VMU compared to that of Ref. [27] by about 55 %. Note that Ref. [27] include only dominant components (see Ref. [11] for the details).

**Table 2.** Calculated cross sections for  $^{40}\text{Ar}(\nu_e, e^-)^{40}\text{K}$  induced by solar  $^8\text{B}$  neutrinos for SDPF-VMU as well as for Ref. [27]. Values are given in units of  $10^{-43} \text{ cm}^2$ .

Hamiltonian	GT	IA	GT + IA
SDPF-VMU	11.95	2.10	14.05
Ref. [27]	7.70	3.80	11.50

## 5 Summary

New neutrino-nucleus cross sections are obtained based on new shell-model Hamiltonians with proper tensor interactions. New Hamiltonians, SFO and GXPF1J, are used for the shell-model calculations of  $p$ -shell and  $pf$ -shell nuclei, respectively. A monopole-based universal interaction, VMU, is used to obtain the  $sd$ - $pf$  cross-shell matrix elements. Experimental cross sections for  $^{12}\text{C}(\nu, e^-)^{12}\text{N}$ ,  $^{12}\text{C}(\nu, \nu')^{12}\text{C}$  and  $^{56}\text{Fe}(\nu, e^-)^{56}\text{Co}$  induced by DAR neutrinos are found to be well reproduced with the new Hamiltonians.

Nucleosynthesis of light elements in supernova explosions is studied using new neutrino-nucleus cross sections on  $^{12}\text{C}$  as well as  $^4\text{He}$ . The enhancement of the abundances of  $^7\text{Li}$  and  $^{11}\text{B}$  is found compared with previous evaluations. The effects of MSW  $\nu$ -oscillations on the abundance ratio of  $^7\text{Li}/^{11}\text{B}$  are investigated. The ratio is found to be sensitive to the oscillation angle  $\theta_{13}$  and the  $\nu$  mass hierarchy. A recent study on supernova grains suggests that the inverted mass hierarchy is statistically more favored.

New  $\nu$  capture cross sections on  $^{13}\text{C}$  are obtained by shell-model calculations with SFO. Charged and neutral-current reaction cross sections leading to low-lying states in  $^{13}\text{N}$  and  $^{13}\text{C}$  are evaluated. The enhancement of the cross sections in GT transitions as well as for solar  $^8\text{B}$  neutrinos are found compared with previous calculations with Cohen-Kurath.  $^{13}\text{C}$  is pointed out to be an attractive target for the detection of very low energy neutrinos. It would help detection of low energy reactor anti- $\nu$  by neutral-current reactions and neutrinos in reactor anti- $\nu$  environment by charged-current reactions.

The GT strength in  $^{56}\text{Ni}$  obtained by GXPF1J has two-peak structure, which has been confirmed by observation. Accurate evaluations of e-capture rates at stellar environments become possible, and hence it is expected to make more reliable estimations of element synthesis such as isotope abundance ratios in Ni isotopes. A larger GT strength  $^{56}\text{Ni}$  at higher excitation energy region is found to lead to larger proton emission cross sections for  $^{56}\text{Ni}$  and production of more  $^{55}\text{Mn}$  in supernova explosions.

The VMU is used to evaluate GT strength in  $^{40}\text{Ar}$ . The GT strength and the cumulative sum of  $B(GT)$  in  $^{40}\text{Ar}$  obtained with VMU are found to be consistent with the experimental data. New charged-current reaction cross sections on  $^{40}\text{Ar}$  are obtained with VMU. The cross section induced by solar  $^8\text{B}$  neutrinos is found to be enhanced compared with previous calculations.

We have shown that we can now evaluate  $\nu$ -induced reaction cross sections such as on  $^{12}\text{C}$  and  $^{56}\text{Fe}$  accurately with the use of new shell-model Hamiltonians. We can, thus, discuss nucleosynthesis in stars,  $\nu$ -oscillation parameters, and detection of solar, reactor and supernova neutrinos with more accuracies and reliabilities. We hope to have further progress in this direction in near future.

The author is grateful to T. Otsuka for collaborations on the work on tensor forces. This work has been supported in part by Grants-in-Aid for Scientific Research No. (C) 22540290 of the MEXT of Japan, and the U.S. National Science Foundation Grant No. PHY-1205024.

## References

- [1] T. Suzuki, R. Fujimoto and T. Otsuka, Phys. Rev. C **67**, 044302 (2003)

- [2] T. Suzuki, S. Chiba, T. Yoshida, T. Kajino and T. Otsuka, *Phys. Rev. C* **74**, 034307 (2006)
- [3] T. Yoshida, T. Suzuki, S. Chiba, T. Kajino, H. Yokomakura, K. Kimura, A. Takamura and D. H. Hartmann, *Astrophys. J.* **686**, 448 (2008)
- [4] T. Suzuki, A. B. Balantekin and T. Kajino, *Phys. Rev. C* **86**, 015502 (2012)
- [5] T. Suzuki and T. Kajino, *J. Phys. G: Nucl. Part. Phys.* **40**, 083101 (2013)
- [6] M. Honma, T. Otsuka, T. Mizusaki, M. Hjorth-Jensen and B. A. Brown, *J. Phys.: Conf. Ser.* **20**, 7 (2005); M. Honma, T. Otsuka, B. A. Brown and T. Mizusaki, *Phys. Rev. C* **65**, 061301 (2002)
- [7] N. Parr, T. Suzuki, M. Honma, T. Marketin and D. Vretenar, *Phys. Rev. C* **84**, 047305 (2011)
- [8] T. Suzuki, M. Honma, K. Higashiyama, T. Yoshida, T. Kajino, T. Otsuka, H. Umeda and K. Nomoto, *Phys. Rev. C* **79**, 061603 (2009)
- [9] M. Sasano et al, *Phys. Rev. Lett.* **107**, 202501 (2012); *ibid.*, *Phys. Rev. C* **86**, 034324 (2012)
- [10] T. Otsuka, T. Suzuki, M. Honma, Y. Utsuno, N. Tsunoda, K. Tsukiyama and M. Hjorth-Jensen, *Phys. Rev. Lett.* **104**, 012501 (2010)
- [11] T. Suzuki and M. Honma, *Phys. Rev. C* **87**, 014607 (2013)
- [12] T. Otsuka, T. Suzuki, R. Fujimoto, H. Grawe and Y. Akaishi, *Phys. Rev. Lett.* **95**, 232502 (2005)
- [13] B. A. Brown, A. Etchegoyen and W. D. M. Rae, The Oxford, Buenos-Aires, Michigan State Shell Model Program (OXBASH) MSU Cyclotron Laboratory Report No. 524 (1986)
- [14] C. Athanassopoulos et al (LSND Collaboration), *Phys. Rev. C* **55**, 2078 (1997); L. B. Auerbach et al (LSND Collaboration), *Phys. Rev. C* **64**, 065501 (2001)
- [15] E. K. Warburton and B. A. Brown, *Phys. Rev. C* **46**, 923 (1992)
- [16] S. E. Woosley, D. H. Hartmann, R. D. Hoffman and W. C. Haxton, *Astrophys. J.* **356**, 272 (1990)  
R. D. Hoffman and S. E. Woosley, Neutrino interaction cross sections and branching ratios, [www.phys.llnl.gov/Research/RRSN/nu\\_csbr/neu\\_rate.html](http://www.phys.llnl.gov/Research/RRSN/nu_csbr/neu_rate.html) (1992)
- [17] K. Abe et al (T2K Collaboration), *Phys. Rev. Lett.* **107**, 041801 (2011); P. Adamson et al (MINOS Collaboration), *Phys. Rev. Lett.* **107**, 181802 (2011); F. An et al (Daya Bay Collaboration), *Phys. Rev. Lett.* **108**, 171803 (2012); Y. Abe et al (Double-Chooz Collaboration), *Phys. Rev. Lett.* **108**, 131801 (2012); J. K. Ahn et al (RENO Collaboration), *Phys. Rev. Lett.* **108**, 191802 (2012)
- [18] W. Fujiya, P. Hoppe and U. Ott, *Astrophys. J.* **730**, L7 (2011)
- [19] G. J. Mathews, T. Kajino, W. Aoki, W. Fujiya and J. B. Pitts, *Phys. Rev. D* **85**, 105023 (2012)
- [20] J. Arafune, M. Fukugita, Y. Kohyama and K. Kubodera, *Phys. Lett. B* **217**, 186 (1989)
- [21] R. Maschuw, *Prog. Part. Nucl. Phys.* **40**, 183 (1998)
- [22] E. Caurier, G. Martinez-Pinedo G. F. Nowacki, A. Poves and A. P. Zuker, *Rev. Mod. Phys.* **77**, 427 (2005)
- [23] T. Suzuki, M. Honma, H. Mao, T. Otsuka and T. Kajino, *Phys. Rev. C* **83**, 044619 (2011)
- [24] L. Iwamoto, F. Brachwitz, K. Nomoto, N. Kishimoto, H. Umeda, W. R. Hix and F. Thielemann, *Astrophys. J. Suppl.* **125**, 439 (1999)
- [25] Y. Utsuno, T. Otsuka, T. Mizusaki and M. Honma, *Phys. Rev. C* **60**, 054315 (1999)
- [26] C. Yuan, T. Suzuki, T. Otsuka, F. Xu and N. Tsunoda, *Phys. Rev. C* **85**, 064324 (2012)
- [27] W. E. Ormand, P. M. Pizzochero, P. F. Bortignon, and R. A. Broglia, *Phys. Lett. B* **345**, 343 (1995)
- [28] M. Bhattacharya, C. D. Goodman, and A. Garcia, *Phys. Rev. C* **80**, 055501 (2009)
- [29] E. Kolbe, K. Langanke, G. Martinez-Pinedo, and P. Vogel, *J. Phys. G* **29**, 2569 (2003); I. Gil-Botella and A. Rubbia, *JCAP* **10**, 9 (2003)